DOI:10.1021/jf903039j

JOURNAL OF AGRICULTURAL AND FOOD CHEMISTRY
ARTICLE

Arginine-Rich Intracellular Delivery Peptides Synchronously Deliver Covalently and Noncovalently Linked Proteins into Plant Cells

Shu-Wan Lu, Jia-Wei Hu, Betty Revon Liu, Cheng-Yi Lee, Jheng-Fong Li, Jyh-Ching Chou, and Han-Jung Lee*

Department of Natural Resources and Environmental Studies, and Institute of Biotechnology, National Dong Hwa University, Hualien 97401, Taiwan

Protein transduction domains (PTDs) are small peptides with a high content of basic amino acids, and they are responsible for cellular uptake. Many PTDs, including arginine-rich intracellular delivery (AID) peptides, have been shown to transport macromolecules across membranes and into cells. In this study, we demonstrated for the first time that AID peptides could rapidly and efficiently deliver proteins into plant cells in both covalent and noncovalent protein transductions (CNPT) simultaneously. The optimal molecular ratio between an AID peptide carrier and cargo in CNPT was about 3:1. Fluorescence resonance energy transfer (FRET) analysis revealed protein−protein interactions between AID peptide carriers and cargos after CNPT in cells. The possible mechanisms of AID peptides-mediated cellular entry might involve a combination of multiple internalization pathways. Therefore, applications by AID peptide-mediated CNPT may provide a simple and direct transport strategy for delivering two proteins in agricultural systems.

KEYWORDS: Cell-penetrating peptide; cellular internalization; fluorescence resonance energy transfer; macropinocytosis; onion; protein transduction domain

INTRODUCTION

Most macromolecules, such as proteins and nucleic acids, are poorly taken up by cells because of the nonpolar barrier of the cell membrane. Over two decades ago, the transactivator of the transcription (Tat) protein of the human immunodeficiency virus type 1 (HIV-1) was found to be able to efficiently enter into cells (*1*, *2*). Subsequent study proved that a short and basic amino acid-rich peptide of the Tat is the functional domain for cellular uptake (*3*). More observations have been reported, and it is concluded that several functional domains for cellular internalization are usually rich in basic amino acids known as the protein transduction domain (PTD) or cell-penetrating peptide (CPP) (*4*). These PTDs could covalently link with a great diversity of cargoes, some even larger than 200 nm in diameter, and traverse the cell membrane (*5*). Cellular uptake of polyarginine tends to be more efficient than that of polylysine, polyhistidine, or polyornithine (*6*). The highest efficiency of cell entrance turned out to be with octa-arginine or nona-arginine (R9) peptides, among various chain lengths of polyarginine (*6*). These results indicated that a high content of arginine can be beneficial for cell penetration ability. We therefore called these kinds of PTDs arginine-rich intracellular delivery (AID) peptides.

The simple and direct delivery of proteins and nucleic acids into plant systems is always in great demand. We found that AID peptides are able to efficiently deliver covalently fused proteins into plant cells (*7*, *8*). Furthermore, we demonstrated that protein transduction can also function in a noncovalent fashion, called noncovalent protein transduction (NPT). AID peptides could efficiently deliver noncovalently mixed proteins (*9*−*13*), RNA (*14*), or DNA (*15*) in active forms into living cells. Despite the controversy and uncertainty of the internalization mechanism of PTD, the potential mechanism of the NPT might involve macropinocytosis (*10*, *12*, *15*). Previous data from our group (*8*−*10*, *12*) and others (*16*, *17*) indicated that the cell wall is not a barrier for the action of protein transduction. The plant tissues studied in our studies are all primary tissues, and therefore, these components are considered simpler than those more complex secondary cell walls. The cutoff sizes of cell walls shall be much higher than 10 kDa at the stage of plant growth. In fact, several proteins and enzymes of cell walls reported are larger than 10 kDa, such as the major wall proteins, expansins, which are around 25−27 kDa (*18*). Moreover, cellular uptake of AID peptides and their cargos could be applied not only in animals and plants but also in bacteria, archaea, and yeasts in a NPT manner (*12*).

Fluorescence resonance energy transfer (FRET) analysis is a powerful method to detect protein−protein interactions and biochemical reactions in living cells (*19*). When the donor molecule is excited, nonradioactive energy transfer can occur from this excited donor fluorescent molecule to another unexcited acceptor fluorescent molecule. Then, the acceptor will emit fluorescence. Finally, the emission spectra of the donor and acceptor will exhibit overlapped fluorescence at the same sites. However, a distance of 1−10 nm between the donor and acceptor is needed while the FRET process occurs (*20*).

*To whom correspondence should be addressed. Telephone: +886-3-8633642. Fax: +886-3-8633260. E-mail: hjlee@mail.ndhu.edu.tw.

 Published on Web 01/21/2010

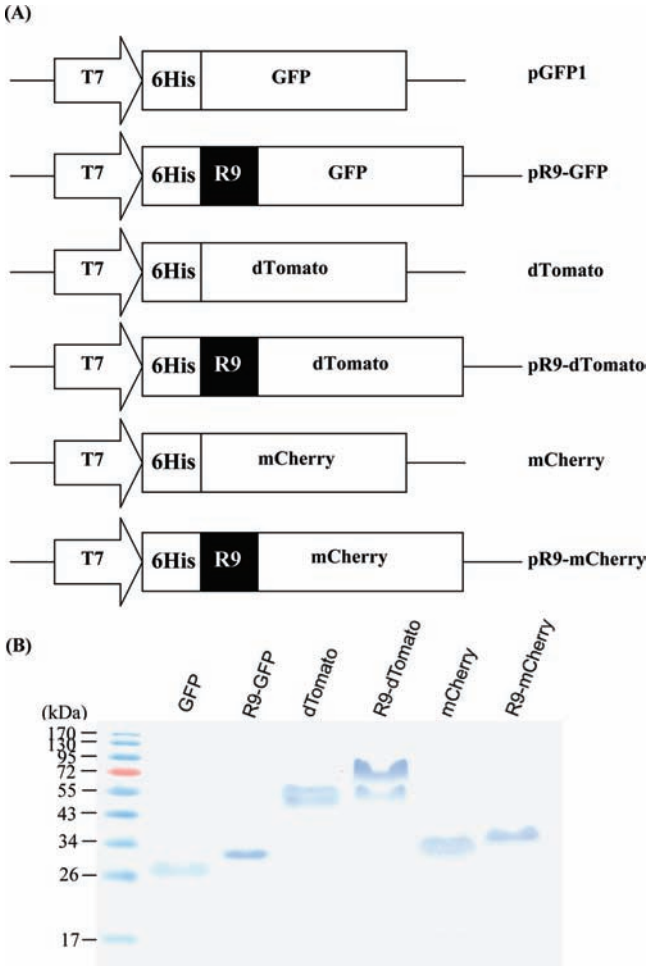

Figure 1. (**A**) Schematic structure of plasmids used in covalent and noncovalent protein transductions (CNPT). Plasmid DNAs mainly contain hexa-histidine (6His)-tagged green fluorescent protein (GFP), nona-arginine (R9)-GFP, dTomato, R9-dTomato, mCherry, and R9-mCherry coding regions under the control of the T7 promoter, respectively. Both dTomato and mCherry encode two red fluorescent protein (RFP) sequences. (**B**) SDS-PAGE analysis of purified FPs from *E. coli* after Coomassie brilliant blue staining. Standard protein molecular masses (SM0671, Fermentas, Burlington, Ontario, Canada) are displayed. Both dTomato and R9-dTomato tend to form dimers (*21*), while GFP (with a calculated molecular mass of 30.4 kDa), R9-GFP (36.7 kDa), mCherry (30.6 kDa), and R9-mCherry (32.6 kDa) remain as monomers.

In this report, we demonstrated that AID peptides could rapidly deliver proteins into plant cells in both covalent and noncovalent protein transductions (CNPT) synchronously. FRET analysis was conducted to reveal protein−protein interactions between AID peptide carriers and cargos after CNPT. Subcellular trackers were used to visualize the potential colocalization of AID peptide carriers in plant cells. Finally, the possible mechanisms of the CNPT might at least involve macropinocytosis.

MATERIALS AND METHODS

Plant Material. Root tips of onion (*Allium cepa* L.) were prepared as previously described (*10*).

Plasmid Constructions. The pGFP1 plasmid was generated by digestion of the pR9-GFP plasmid with *Nhe*I and *Nco*I restriction enzymes to remove the R9 coding region, followed by blunting of the ends and self-ligation. pR9-GFP, dTomato, and mCherry plasmids were described previously (*13*, *21*). In brief, the pR9-GFP plasmid contains the hexa-histidine (6His), R9 tags, and green fluorescent protein (GFP) coding regions under the control of the T7 promoter. Both dTomato and mCherry plasmids (kindly provided by Dr. Roger Y. Tsien, University of California, San Diego, CA) consist of red fluorescent protein (RFP) coding sequences under the control of the T7 promoter (*21*). The pR9-RFP plasmid (*7*) was digested with *Nhe*I and *Bgl*II restriction enzymes to generate the pR9-RFPW plasmid. The pR9-II vector was constructed by the digestion of this pR9-RFPW plasmid with *Kpn*I restriction enzyme to delete the DsRed coding sequence, the bluntness of both ends, and the self-ligation. Both pR9-dTomato and pR9-mCherry plasmids were generated by the insertion of dTomato and mCherry coding regions from dTomato and mCherry plasmids into the *Bam*HI and *Hind*III sites of the pR9-II vector, respectively. All constructs were confirmed by DNA sequencing.

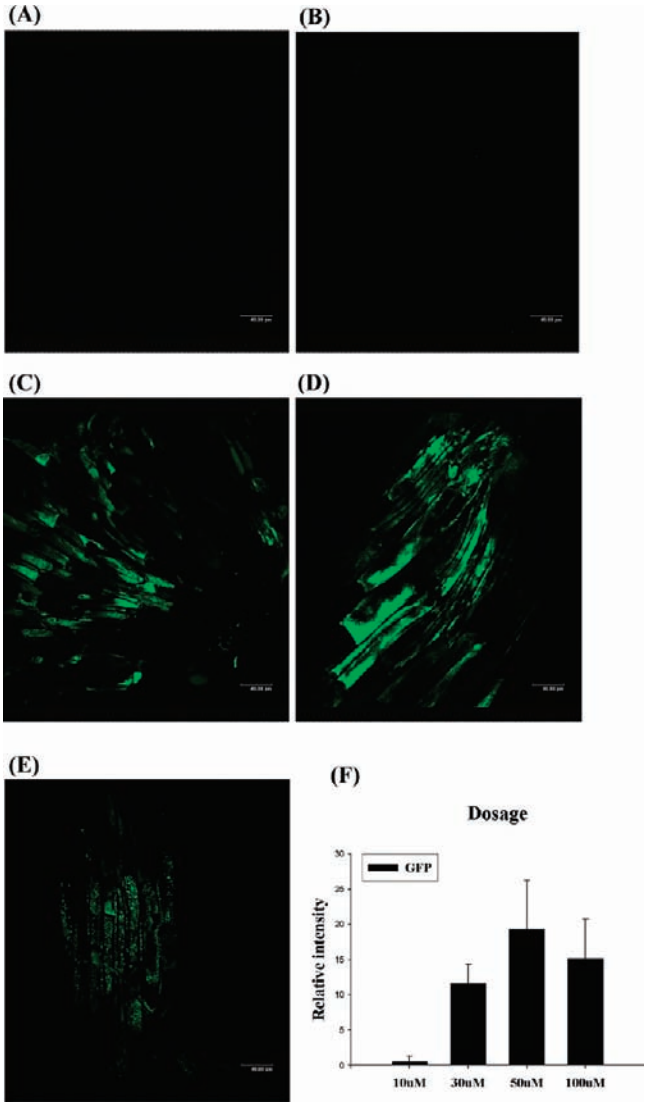

Figure 2. Dosage-response study of covalent protein transduction (CPT). Onion cells were treated with GFP (**A**), 10 (**B**), 30 (**C**), 50 (**D**), or 100 (**E**) μM of R9-GFP at room temperature for 20 min. Fluorescent images were recorded with a confocal microscope, and relative intensity (**F**) was quantified with the UN-SCAN-IT software. The scale bar is 40 μm.

Protein Preparation and SDS-PAGE Analysis. Plasmids were transformed into the *Escherichia coli* KRX strain (Promega, Madison, WI). Protein expression and purification were described previously with relevant modifications (*22*). Bacteria were grown until the OD_{600} reached 0.5, and rhamnose (Sigma-Aldrich, St. Louis, MO) was added to the final concentration of 0.05% (w/v) at 25 °C (*13*). Finally, purified proteins were concentrated by Microsep 10K concentrators (Filtron, Northborough, MA) and quantified by the Protein Assay Kit (Bio-Rad, Hercule, CA). SDS-PAGE analysis was employed as previously described (*22*).

Covalent and Noncovalent Protein Transductions (CNPT). Intact root tips of onion were washed with double distilled water two times. To test the optimal concentration of covalent protein transduction (CPT),

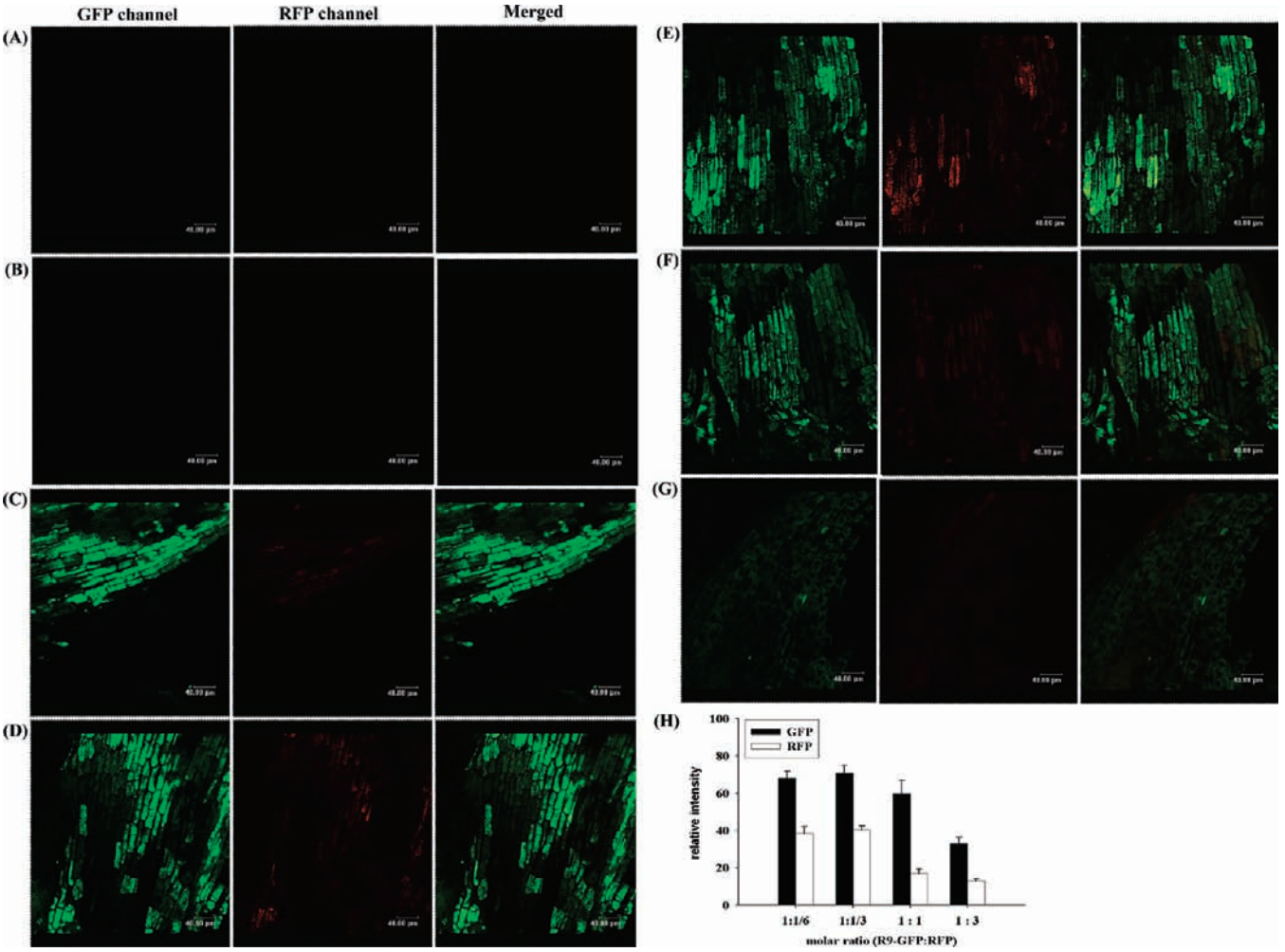

Figure 3. Confocal microscopy of covalent and noncovalent protein transductions (CNPT) with R9-GFP/RFP. Onion root tip cells were treated with dTomato (**A**), GFP (**B**), R9-GFP (**C**), 1:1/6 (**D**), 1:$^1/_3$ (**E**), 1:1 (**F**), or R9-GFP and RFP (dTomato) mixtures in a molecular ratio of 1:3 (**G**) in a total volume of 50 μL for 20 min at room temperature. Images were recorded with a confocal microscope in the GFP (500−530 nm), RFP (580−650 nm), and GFP/RFP merged channels, respectively. The scale bar is 40 μm. The relative intensity from the treatment of R9-GFP and RFP mixtures was summarized (**H**).

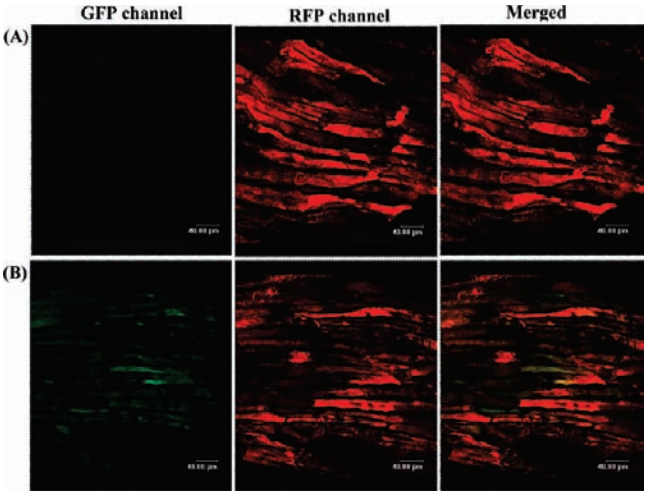

Figure 4. Confocal microscopy of covalent and noncovalent protein transductions (CNPT) with R9-RFP/GFP. Onion root tips were treated with R9-dTomato (**A**) or R9-RFP (R9-dTomato) and GFP mixtures in a molecular ratio of 1:$^1/_3$ (**B**) for 20 min at room temperature. Images were recorded with a confocal microscope in the GFP (500−530 nm), RFP (580−650 nm), and GFP/RFP merged channels, respectively. The scale bar is 40 μm.

root tips were treated with R9-GFP at final concentrations of 10, 30, 50, and 100 μM for 20 min and washed with water in order to remove any proteins on the surface of toot tips as previously described (*10*). For dual color analysis, root tips were treated with 50 μM GFP or RFP [68 μg of fluorescent protein (FP) in the sample volume of 50 μL] for 20 min and washed with water as a control at room temperature. To test CNPT (*13*), 50 μM R9-GFP was premixed with various concentrations of RFP at molar ratios (R9-GFP:RFP) of 1:$^1/_6$, 1:$^1/_3$, 1:1, and 1:3 at room temperature for 10 min. When both green and red colors colocalized in a certain area, the merged signal appeared in yellow. Root tips were treated with R9-GFP and RFP mixtures for 20 min and washed with water. In contrast, FP partners of carrier and cargo were switched in CNPT. Fifty micromolar R9-RFP was premixed with 16.7 μM GFP (at the molar ratio of 1:$^1/_3$) at room temperature for 10 min. Root tips were then treated with R9-RFP and GFP mixtures for 20 min.

Fluorescence Resonance Energy Transfer (FRET) Assay. Root tips were treated with 50 μM of R9-GFP and 16.7 μM of mCherry (at the molar ratio of 1:$^1/_3$) for 10 min. After the treatment of CNPT, cells of root tips were detected with the TCS SL confocal microscope system (Leica, Wetzlar, Germany) as previously described (*10*, *13*). We set the wavelength of excitation at 488 nm and emission at 500−530 nm and 620−700 nm bandpass barrier filter. Under these conditions, GFP, but not mCherry, could be excited by light with the wavelength at 488 nm. FRET efficiency representing the fraction of energy transfer per donor excitation was calculated pixel-by-pixel by the AccPbFRET program, an ImageJ (1.42q version, NIH, USA) plugin for semiautomatic and fully corrected analysis of FRET images (*23*).

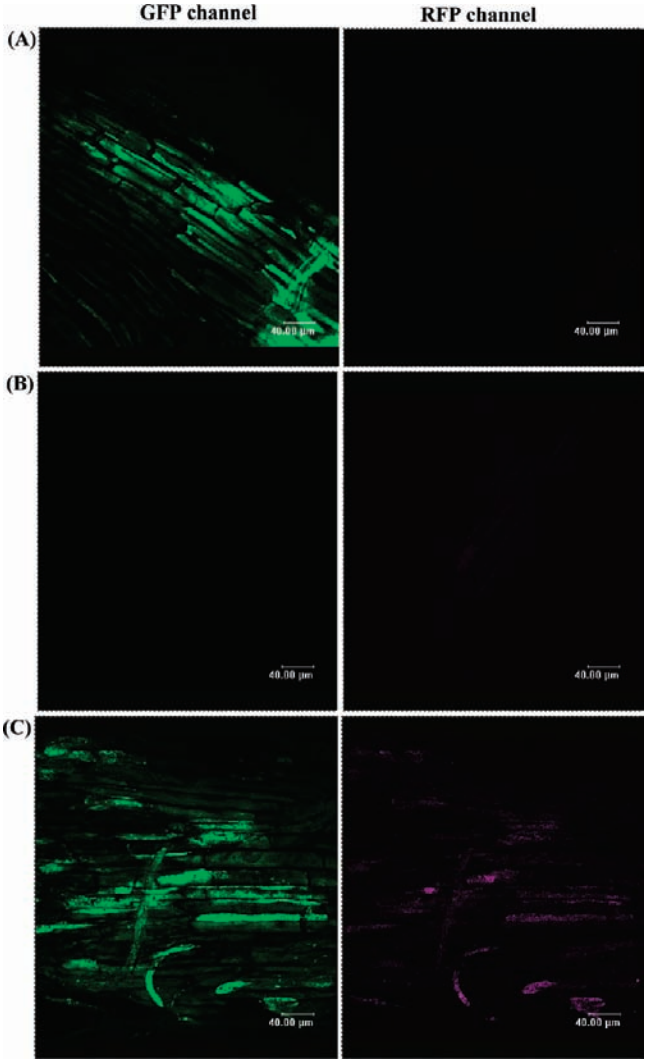

Figure 5. Analysis of protein−protein interactions in covalent and noncovalent protein transductions (CNPT) by fluorescence resonance energy transfer (FRET). Onion root tips were treated with R9-GFP (**A**), R9-mCherry (**B**), or R9-GFP and RFP (mCherry) mixtures in a 1:$^1/_3$ molecular ratio (**C**) for 20 min at room temperature. Images were recorded with a confocal microscope with excitation at 488 nm only and emission in the GFP (500−530 nm) and RFP (620−700 nm) channels, respectively. The scale bar is 40 μm.

Confocal and Fluorescent Microscopy. Fluorescent images were recorded with the TCS SL confocal microscopy system (Leica) as previously described (*10*). For the GFP channel, we set excitation at 488 nm and emission at 500−530 nm bandpass barrier filters. For the RFP channel, we set excitation at 543 nm and emission at 580−650 nm. For the mCherry channel, we set excitation at 543 nm and emission at 620−700 nm. The relative intensity of the fluorescent image was quantified by the UN-SCAN-IT software (Silk Scientific, Orem, UT) as previously described (*9*). Fluorescent images of subcellular colocalization analysis were detected by the Olympus IX70 inverted fluorescent microscope (Olympus, Center Valley, PA) using a UPLFLN 60X NA 1.25 objective with WU, WB, and WG filters (Brightline, Bridgeville, PA). For the GFP channel, we set excitation at 460−490 nm and emission at 520 nm. For the RFP channel, we set excitation at 510−550 nm and emission at 590 nm. For the blue fluorescent protein (BFP) channel, we set excitation at 330−385 nm and emission at 420 nm. Images were captured with a Hamamatsu ORCA285 CCD camera. Shutters, filters, and the camera were controlled with the SlideBook software (Intelligent Imaging Innovations, Denver, CO).

Subcellular Colocalization Analysis. MitoTracker Deep Red FM (Invitrogen, Carlsbad, CA) is a mitochondrial probe, LysoTracker Red DND-99 (Invitrogen) is a probe to detect the acidic autolysosome and lysosome-like vesicles by the RFP channel, and Hoechst 33342 (Invitrogen) is a nuclear probe detected by the BFP channel in living plant cells (*13*). Root tips were treated with 195 μM of Hoechst and either 500 nM of MitoTracker or 75 nM of LysoTracker for 2 h at room temperature according to the manufacturer's instructions and followed by the treatment with 50 μM of R9-GFP for an additional 20 min. After treatment, mitochondria and lysosomes would exhibit red signals in cells, nuclei were in blue, and R9-GFP proteins were in green, detected by the Olympus IX70 fluorescent microscope. When both R9-GFP and trackers colocalized in a certain area, the merged signal appeared in yellow.

Mechanisms of Cellular Internalization. To reveal mechanisms of cellular uptake, root tip cells were treated with 50 μM of R9-dTomato and 16.7 μM of GFP (at the molar ratio of 1:$^1/_3$) for 10 min in the presence or absence of various treatments or chemical inhibitors. For energy-independent experiments, root tips were pretreated at 4 °C for 30 min prior to the treatment of R9-RFP and GFP mixtures as previously described (*10*). For macropinocytosis and F-actin rearrangement assays, plant cells were treated with R9-RFP and GFP mixtures in the presence or absence of 100 μM of 5-(*N*-ethyl-*N*-isopropyl)amiloride (EIPA; Sigma-Aldrich) and 10 μM of cytochalasin D (CytD; Sigma-Aldrich) for 30 min, respectively (*10*). For the cellular membrane binding assay, root tips were treated with 80 mM of sodium chlorate ($NaClO_3$; Sigma-Aldrich) for 24 h (*24*) prior to the treatment of R9-RFP and GFP mixtures. For the cellular motion assay, root tips were treated with 2 mM of methyl-β-cyclodextrin (MβCD; Sigma-Aldrich) for 30 min (*24*) or 10 μM of nocodazole (Sigma-Aldrich) for 2 h (*25*) before the treatment of R9-RFP and GFP mixtures. Relative intensities were analyzed by the UN-SCAN-IT software from confocal microscopic images.

Statistical Analysis. Results were expressed as means ± standard deviations. Statistical comparisons between the control and treated groups were performed by the Student's *t*-test. Means and standard deviations were calculated for each sample assayed at least in triplicate. The levels of statistical significance were set at $P < 0.05$ (*) or 0.01 (**).

RESULTS AND DISCUSSION

Plasmid Constructions and Protein Preparation. To study CNPT in plant cells, we prepared and constructed several plasmids (**Figure 1A**). GFP, R9-GFP, dTomato, R9-dTomato, mCherry, and R9-mCherry proteins were overexpressed in the *E. coli* KRX strain transformed with pGFP1, pR9-GFP, dTomato, pR9-dTomato, mCherry, and pR9-mCherry plasmids, respectively (**Figure 1B**). Both GFP and RFP (such as dTomato and mCherry) are FPs, while R9-GFP, R9-dTomato, and R9-mCherry are fusion proteins with R9 tags in addition to FPs.

Covalent and Noncovalent Protein Transductions (CNPT). To determine the optimal concentration of AID peptides in CPT, onion root tip cells were treated with different concentrations of GFP protein or R9-GFP fusion protein for 20 min. As shown in **Figure 2A**, no fluorescence could be detected in root tip cells treated with GFP alone. In contrast, cells incubated with 10 (**Figure 2B**), 30 (**Figure 2C**), 50 (**Figure 2D**), and 100 (**Figure 2E**) μM of R9-GFP exhibited green fluorescence. The maximal fluorescent intensity was reached when 50 μM of R9-GFP was applied (**Figure 2F**). Interestingly, we found 100 μM of AID peptides in CPT did not further increase the efficiency of cellular uptake when compared with that in 50 μM of AID peptides (panels **D** and **E** of **Figure 2**). It has been suggested that the use of PTD concentrations should be done at or less than 100 μM, as concentrations above this dose tend to cause toxicity (*7*, *10*, *15*, *26*). Thus, lower concentrations of protein content should be considered in the application of CNPT.

To find out the optimal molecular ratio between R9-GFP and dTomato, root tip cells were treated with 50 μM of R9-GFP noncovalently mixed with different concentrations of dTomato. The various molecular ratios of R9-GFP:dTomato were 1:1/6, 1:$^1/_3$, 1:1, and 1:3 (**Figure 3**). There was no signal in root tips treated with dTomato and GFP (panels **A** and **B** of **Figure 3**). Green fluorescence was detected in root tip cells treated with

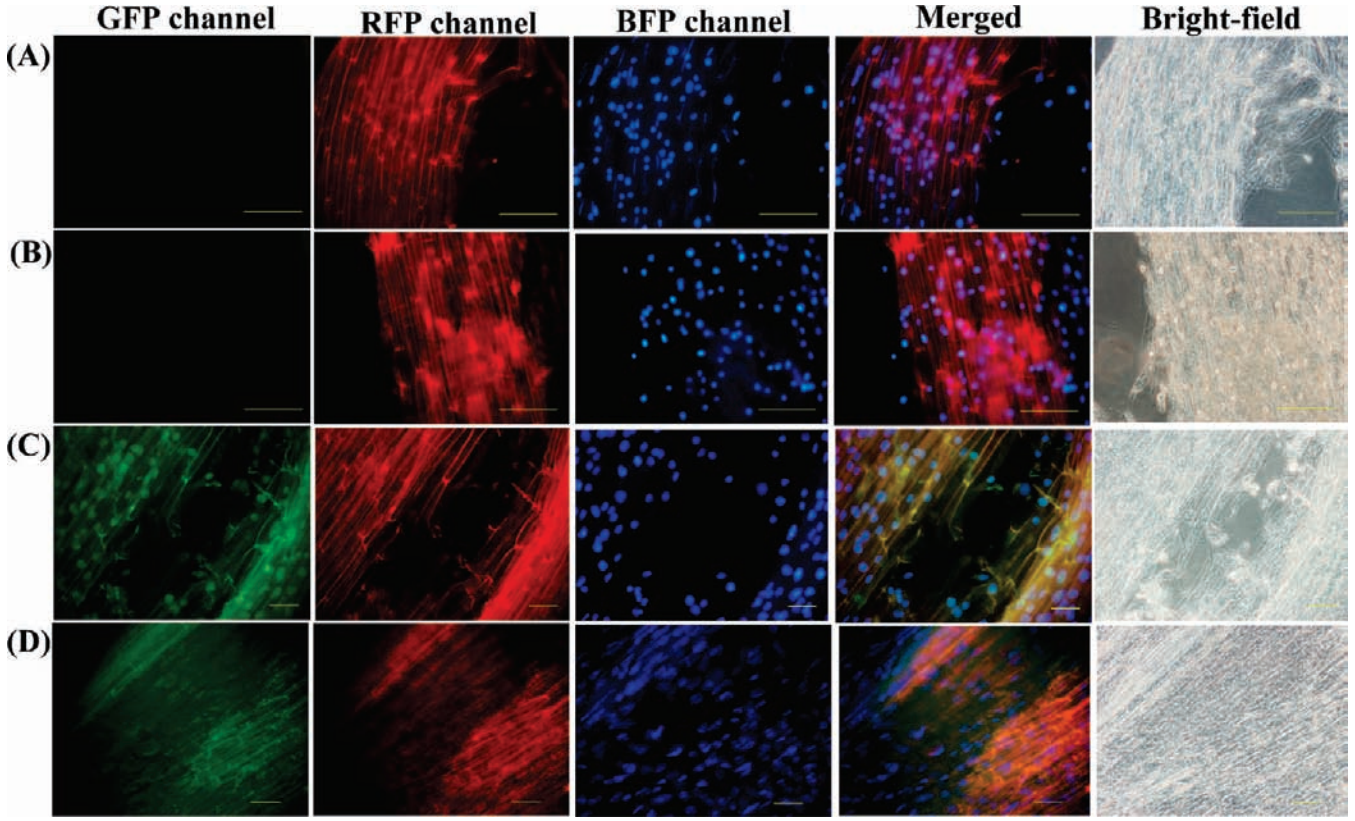

Figure 6. Analysis of the colocalization of arginine-rich intracellular delivery (AID) peptides. Onion root tips were treated with 195 μM of Hoechst and either 500 nM of MitoTracker (**A**) or 5 nM of LysoTracker (**B**) for 2 h at room temperature. Root tips were then incubated with 50 μM of R9-GFP for 20 min at room temperature after treatment of Hoechst and either MitoTracker (**C**) or LysoTracker (**D**). Images were recorded with a fluorescent microscope in the GFP (520 nm), RFP (590 nm), BFP (420 nm), and GFP/RFP/BFP merged channels and bright-field view, respectively. The scale bar is 10 μm.

R9-GFP (**Figure 3C**). Interestingly, both green and red fluorescent images were detected in root tip cells treated with R9-GFP and dTomato mixtures (panels **D**−**G** of **Figure 3**). In summary, more effective CNPT were observed when the molecular ratio of R9-GFP:dTomato was 1:$^1/_3$ (**Figure 3H**). These results indicated that AID peptides not only transport covalently linked GFP proteins into cells by themselves but also deliver noncovalently linked RFPs into cells synchronously. Moreover, the optimal molecular ratio between R9-GFP carrier and RFP cargo in CNPT was about 3:1.

To extend CNPT mediated by R9 peptides to other proteins, we switched the FP partners of carrier and cargo in the dual color system. Red, but not green, fluorescence was detected in root tip cells treated with R9-dTomato (**Figure 4A**). In contrast, cells treated with R9-dTomato and GFP mixtures at the molecular ratio (R9-dTomato:GFP) of 1:$^1/_3$ exhibited both green and red fluorescent images (**Figure 4B**). These results confirmed again that AID peptides are able to deliver different proteins in living plant cells in CNPT.

Protein−**Protein Interactions in CNPT.** It shall be noticed that both dTomato and mCherry are RFPs with slightly different emission wavelengths (*21*). In this study, we used either the R9-GFP/RFP or R9-RFP/GFP pair to demonstrate the CNPT where the RFP is dTomato. However, the characteristics of dTomato, particularly its obligate dimerization (*21*), impede its application in FRET (*19*). The GFP/mCherry pair was proved to be an accurate FRET measurement (*19*). Therefore, we replaced dTomato with mCherry and applied the improved and accurate R9-GFP/mCherry pair in FRET experiments.

To study protein−protein interactions after CNPT in cells, we used mCherry as the red fluorescent reporter and conducted the fluorescent protein-based FRET analysis. In FRET experiments, we set excitation at 488 nm and the emission at 500−530 nm for the GFP channel and 620−700 nm for the RFP channel. As shown in **Figure 5A**, root tips treated with R9-GFP clearly exhibited green, but not red, fluorescence. However, no fluorescence was detected in root tips treated with mCherry (data not shown) or R9-mCherry (**Figure 5B**) alone when excited at 488 nm. This is important to show the acceptor fluorophore cannot be excited directly with the wavelength of light that is chosen to excite the donor fluorophore in FRET (*19*, *20*). In contrast, root tips treated with R9-GFP and mCherry mixtures exhibited both green and purple fluorescence when excited at 488 nm (**Figure 5C**). The FRET efficiency between R9-GFP and mCherry was 10.8%, calculated from one time experiment. These results suggested that AID peptides physically interact with their cargo RFPs after CNPT in cells.

Subcellular Colocalization of AID Peptides. The cellular localization of AID peptides tends to stay in cytosol based on results of R9-FP from **Figures 2**−**5**. To detect the colocalization of AID peptides, root tips were treated with MitoTracker, LysoTracker, and Hoechst to specifically detect the mitochondrium, lysosome, and nucleus, respectively. Root tips were treated with Hoechst and either MitoTracker (**Figure 6A**) or LysoTracker (**Figure 6B**) before the treatment of R9-GFP. In the presence of R9-GFP, colocalization of R9-GFP was partially involved in mitochondria (**Figure 6C**), lysosomes (**Figure 6D**), and nuclei (panels **C** and **D** of **Figure 6**). These results suggested that AID peptides mainly remain in cytosol during CNPT in cells.

Mechanisms of Cellular Entry of AID Peptide-Mediated CNPT. To study the potential mechanisms of CNPT, experiments were performed in the presence or absence of treatment or inhibitors. Clathrin- and caveolae-dependent endocytosis needs dynamin

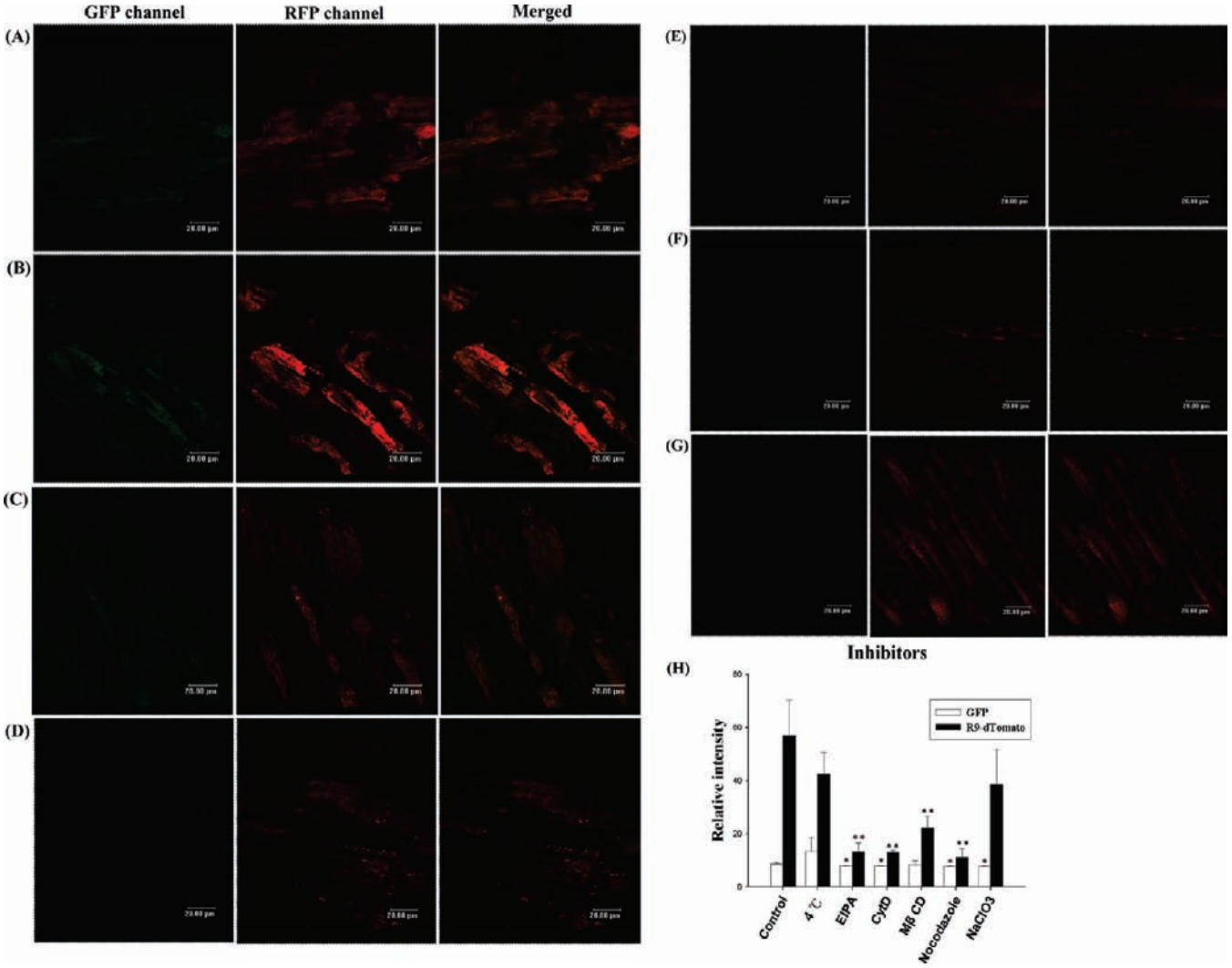

Figure 7. Analysis of mechanisms of covalent and noncovalent protein transductions (CNPT). Onion root tips were treated with R9-dTomato and GFP mixtures in the absence (**A**) or presence of 4 °C (**B**), EIPA (**C**), CytD (**D**), MβCD (**E**), nocodazole (**F**), or $NaClO_3$ (**G**) for 20 min at room temperature. Images were recorded with a confocal microscope in the GFP (500−530 nm), RFP (580−650 nm), and GFP/RFP merged channels, respectively. The scale bar is 20 μm. Relative intensity was summarized (H).

GTPase activity to form vesicles at the cell membrane, but macropinocytosis does not require energy for endocytosis (*27*). In the 4 °C treatment, all energy-dependent molecular movements are believed to be inhibited (*28*). Root tip cells were treated with R9-dTomato and GFP mixtures in the absence of any treatment or inhibitors (**Figure 7A**). Cells were treated with 4 °C before and during the treatment of R9-RFP and GFP mixtures. We found low temperature incubation did not remarkably alter cellular uptake (panels of **B** and **H** of **Figure 7**), which excludes the energy-dependent mechanism.

Although the action of AID peptides was not inhibited at 4 °C, cellular uptake via macropinocytosis involving formation of macropinosomes and the actin cytoskeleton can be greatly affected by the macropinocytosis inhibitor EIPA and the F-actin polymerization inhibitor CytD (*29*). We found treatment of these two inhibitors resulted in a dramatic reduction in cellular entry (panels of **C**, **D**, and **H** of **Figure 7**). These results suggested that AID-peptide mediated CNPT involved macropinocytosis and actin rearrangement.

To investigate the possible role of cellular motion in CNPT, MβCD, which sequesters cholesterol from the plasma membrane (*24*), and nocodazole, which inhibited microtubule polymerization (*25*), were used to assay cellular motion. As shown in panels **E**, **F**, and **H** of **Figure 7**, we found significant inhibitions in cellular uptake when cells were treated with cellular motion inhibitors. These results indicated that AID peptide-mediated CNPT involved cellular motion and microtubule polymerization.

Since the sulfate groups of proteoglycans provide a dense region of negative charge on the cell surface, sodium chlorate, which removes sulfate groups of negatively charged proteoglycans (*30*), was applied in CNPT. No significant difference was detected in CPT, but a significant difference was detected in NPT (panels **G** and **H** of **Figure 7**). These results implied that cellular binding to proteoglycans may play an important role in NPT but not in CPT.

The mechanism of cellular uptake mediated by a PTD is still controversial. We also realize that treatments or inhibitors applied in CNPT have their limitations and complexities in order to interpret possible mechanisms. Nevertheless, our present results indicated that AID peptides-mediated CNPT may involve an energy-independent pathway, macropinocytosis, F-actin, and microtubule polymerization (**Figure 7**). Moreover, detailed study from sodium chlorate treatment suggested that CNPT, composed of CPT and NPT parts, showed different preferences toward cellular binding qof proteoglycans. Together, these results are in agreement with very recent reviews (*4*, *31*). A variety of endocytic (clathrin- and caveolin-dependent) mechanisms and macropinocytosis has been

suggested (*4*). We therefore proposed that potential uptake mechanisms of cargos mediated by AID peptides in CNPT involve a combination of multiple internalization pathways.

In conclusion, the present study is the first report demonstrating that AID peptides were proved to not only deliver covalently conjugated proteins into plant cells but also shuttle noncovalently mixed proteins into cells simultaneously. In recent years, vast amounts of diverse cargos delivered by PTD-mediated cellular uptake have been accumulated (*5*). These cargos include proteins, nucleic acids, peptide nucleic acids (PNAs), nanoparticles, and liposomes, for instance. Our results of CNPT presented herein have provided a powerful tool for delivering two proteins or compounds at the same time by AID peptide-mediated cellular internalization. Therefore, applications in CNPT may supply a simple and direct transport strategy for delivering proteins or nucleic acids into plant systems.

ABBREVIATIONS USED

AID, arginine-rich intracellular delivery; BFP, blue fluorescent protein; CNPT, covalent and noncovalent protein transductions; CPP, cell-penetrating peptide; CPT, covalent protein transduction; CytD, cytochalasin D; EIPA, 5-(*N*-ethyl-*N*-isopropyl)amiloride; FP, fluorescent protein; FRET, fluorescence resonance energy transfer; GFP, green fluorescent protein; 6His, hexa-histidine; MβCD, methyl-β-cyclodextrin; NPT, noncovalent protein transduction; PTD, protein transduction domain; R9, nona-arginine; RFP, red fluorescent protein; TAT, transactivator of transcription.

ACKNOWLEDGMENT

We thank Dr. Roger Y. Tsien for provision of both dTomato and mCherry plasmids.

LITERATURE CITED

(1) Green, M.; Loewenstein, P. M. Autonomous functional domains of chemically synthesized human immunodeficiency virus Tat transactivator protein. *Cell* **1988**, *55*, 1179–1188.
(2) Frankel, A. D.; Pabo, C. O. Cellular uptake of the Tat protein from human immunodeficiency virus. *Cell* **1988**, *55*, 1189–1193.
(3) Vives, E.; Brodin, P.; Lebleu, B. A truncated HIV-1 tat protein basic domain rapidly translocates through the plasma membrane and accumulates in the cell nucleus. *J. Biol. Chem.* **1997**, *272*, 16010–16017.
(4) Nakase, I.; Takeuchi, T.; Tanaka, G.; Futaki, S. Methodological and cellular aspects that govern the internalization mechanisms of arginine-rich cell-penetrating peptides. *Adv. Drug Delivery Rev.* **2008**, *60*, 598–607.
(5) Wadia, J. S.; Dowdy, S. F. Protein transduction technology. *Curr. Opin. Biotechnol.* **2002**, *13*, 52–56.
(6) Futaki, S. Arginine-rich peptides: potential for intracellular delivery of macromolecules and the mystery of the translocation mechanisms. *Int. J. Pharm.* **2002**, *245*, 1–7.
(7) Chang, M.; Chou, J. C.; Lee, H. J. Cellular internalization of fluorescent proteins via arginine-rich intracellular delivery peptide in plant cells. *Plant Cell Physiol.* **2005**, *46*, 482–488.
(8) Liu, K.; Lee, H. J.; Leong, S. S.; Liu, C. L.; Chou, J. C. A bacterial indole-3-acetyl-L-aspartic acid hydrolase inhibits mung bean (*Vigna radiata* L.) seed germination through arginine-rich intracellular delivery. *J. Plant Growth Regul.* **2007**, *26*, 278–284.
(9) Wang, Y. H.; Chen, C. P.; Chan, M. H.; Chang, M.; Hou, Y. W.; Chen, H. H.; Hsu, H. R.; Liu, K.; Lee, H. J. Arginine-rich intracellular delivery peptides noncovalently transport protein into living cells. *Biochem. Biophys. Res. Commun.* **2006**, *346*, 758–767.
(10) Chang, M.; Chou, J. C.; Chen, C. P.; Liu, B. R.; Lee, H. J. Noncovalent protein transduction in plant cells by macropinocytosis. *New Phytol.* **2007**, *174*, 46–56.
(11) Hou, Y. W.; Chan, M. H.; Hsu, H. R.; Liu, B. R.; Chen, C. P.; Chen, H. H.; Lee, H. J. Transdermal delivery of proteins mediated by noncovalently associated arginine-rich intracellular delivery peptides. *Exp. Dermatol.* **2007**, *16*, 999–1006.
(12) Liu, B. R.; Chou, J. C.; Lee, H. J. Cell membrane diversity in noncovalent protein transduction. *J. Membr. Biol.* **2008**, *222*, 1–15.
(13) Hu, J. W.; Liu, B. R.; Wu, C. Y.; Lu, S. W.; Lee, H. J. Protein transport in human cells mediated by covalently and noncovalently conjugated arginine-rich intracellular delivery peptides. *Peptides* **2009**, *30*, 1669–1678.
(14) Wang, Y. H.; Hou, Y. W.; Lee, H. J. An intracellular delivery method for siRNA by an arginine-rich peptide. *J. Biochem. Biophys. Methods* **2007**, *70*, 579–586.
(15) Chen, C. P.; Chou, J. C.; Liu, B. R.; Chang, M.; Lee, H. J. Transfection and expression of plasmid DNA in plant cells by an arginine-rich intracellular delivery peptide without protoplast preparation. *FEBS Lett.* **2007**, *581*, 1891–1897.
(16) Unnamalai, N.; Kang, B. G.; Lee, W. S. Cationic oligopeptide-mediated delivery of dsRNA for post-transcriptional gene silencing in plant cells. *FEBS Lett.* **2004**, *566*, 307–310.
(17) Chugh, A.; Eudes, F. Study of uptake of cell penetrating peptides and their cargoes in permeabilized wheat immature embryos. *FEBS J.* **2008**, *275*, 2403–2414.
(18) Shcherban, T. Y.; Shi, J.; Durachko, D. M.; Guiltinan, M. J.; McQueen-Mason, S. J.; Shieh, M.; Cosgrove, D. J. Molecular cloning and sequence analysis of expansins−a highly conserved, multigene family of proteins that mediate cell wall extension in plants. *Proc. Natl. Acad. Sci. U.S.A.* **1995**, *92*, 9245–9249.
(19) Tramier, M.; Zahid, M.; Mevel, J. C.; Masse, M. J.; Coppey-Moisan, M. Sensitivity of CFP/YFP and GFP/mCherry pairs to donor photobleaching on FRET determination by fluorescence lifetime imaging microscopy in living cells. *Microsc. Res. Tech.* **2006**, *69*, 933–939.
(20) Piston, D. W.; Kremers, G. J. Fluorescent protein FRET: the good, the bad and the ugly. *Trends Biochem. Sci.* **2007**, *32*, 407–414.
(21) Shaner, N. C.; Campbell, R. E.; Steinbach, P. A.; Giepmans, B. N. G.; Palmer, A. E.; Tsien, R. Y. Improved monomeric red, orange and yellow fluorescent proteins derived from *Discosoma* sp. red fluorescent protein. *Nat. Biotechnol.* **2004**, *22*, 1567–1572.
(22) Chang, M.; Hsu, H. Y.; Lee, H. J. Dye-free protein molecular weight markers. *Electrophoresis* **2005**, *26*, 3062–3068.
(23) Roszik, J.; Szollosi, J.; Vereb, G. AccPbFRET: an ImageJ plugin for semi-automatic, fully corrected analysis of acceptor photobleaching FRET images. *BMC Bioinf.* **2008**, *9*, 346.
(24) Hess, G. T.; Humphries, W. H.; Fay, N. C.; Payne, C. K. Cellular binding, motion, and internalization of synthetic gene delivery polymers. *Biochim. Biophys. Acta* **2007**, *1773*, 1583–1588.
(25) Drin, G.; Cottin, S.; Blanc, E.; Rees, A. R.; Temsamani, J. Studies on the internalization mechanism of cationic cell-penetrating peptides. *J. Biol. Chem.* **2003**, *278*, 31192–31201.
(26) Jones, S. W.; Christison, R.; Bundell, K.; Voyce, C. J.; Brockbank, S. M.; Newham, P.; Lindsay, M. A. Characterization of cell-penetrating peptide-mediated peptide delivery. *Br. J. Pharmacol.* **2005**, *45*, 1093–1102.
(27) Jones, A. T. Macropinocytosis: searching for an endocytic identity and role in the uptake of cell penetrating peptides. *J. Cell. Mol. Med.* **2007**, *11*, 670–684.
(28) Kaplan, I. M.; Wadia, J. S.; Dowdy, S. F. Cationic TAT peptide transduction domain enters cells by macropinocytosis. *J. Controlled Release* **2005**, *102*, 247–253.
(29) Nakase, I.; Niwa, M.; Takeuchi, T.; Sonomura, K.; Kawabata, N.; Koike, Y.; Takehashi, M.; Tanaka, S.; Ueda, K.; Simpson, J. C.; Jones, A. T.; Sugiura, Y.; Futaki, S. Cellular uptake of arginine-rich peptides: roles for macropinocytosis and actin rearrangement. *Mol. Ther.* **2004**, *10*, 1011–1022.
(30) Rabenstein, D. L. Heparin and heparan sulfate: structure and function. *Nat. Prod. Rep.* **2002**, *19*, 312–331.
(31) El-Sayed, A.; Futaki, S.; Harashima, H. Delivery of macromolecules using arginine-rich cell-penetrating peptides: ways to overcome endosomal entrapment. *AAPS J.* **2009**, *11*, 13–22.

Received for review September 1, 2009. Revised manuscript received January 5, 2010. Accepted January 5, 2010. This work was supported by the National Science Council (NSC 97-2621-B-259-003-MY3 to H.-J.L.), Taiwan.